Dry reforming of methane under mild conditions using radio frequency plasma

Edwin Devid,*[a], Diyu Zhang[a,b], Dongping Wang[a], Maria Ronda-Lloret[c], Qiang Huang[a,d], Gadi Rothenberg[c], N. Raveendran Shiju[c], Aart W. Kleyn*[a]

Abstract:

Dry reforming of methane is a challenging process wherein methane reacts with CO_2 to give syngas. This reaction is strongly endothermic, typically requiring temperatures higher than 500 °C. Catalysts can be used, but the high temperatures (which are a thermodynamic requirement) often lead to catalyst deactivation. Here, we approach the reaction from another conceptual direction, using low-power radio frequency inductively coupled plasma (RF-ICP). We demonstrate that this system can give high conversions of methane and CO_2 at near-ambient temperatures. Importantly, the energy costs in this system are considerably lower compared to other plasma-driven DRM processes. Furthermore, we show that the yield of hydrogen can be increased by minimizing the C2 compound formation. We examine the factors that govern the DRM process and discuss the H_α emission and its influence on the H-atom recycling in the process.

Introduction

The effects of climate change caused by greenhouse gases are numerous and include deglaciation, marine heatwaves and threats to global biodiversity. [1-3] Carbon dioxide and methane are the most important anthropogenic greenhouse gases both by volume and by their contribution to the greenhouse effect. Ideally, society should stop emitting these gases completely, and hopefully this will be done in the future (see e.g. the Sky scenario [4]). Meanwhile, we should focus research on approaches for minimizing the impact of methane and CO_2 and removing them from the atmosphere. This means that we also need chemical reactions that consume methane, without generating CO_2. One such possibility is the so-called dry reforming of methane (DRM: $CH_4+CO_2 \rightarrow 2CO+2H_2$). In this process, carbon dioxide and methane react to give syngas, a mixture of H_2 and CO, which can then be converted via Fischer-Tropsch synthesis into valuable hydrocarbon products. [5-6]

DRM is a strongly endothermic reaction, with ΔH^0 = 2.56 eV or +247 kJ mol^{-1}. High temperatures (>500 °C) are needed to shift the equilibrium to the products side. However, such high temperatures mean very costly equipment and often cause catalyst deactivation via sintering and/or coking, see e.g. [7-8]. Running the DRM process at lower temperatures is therefore a worthy scientific and technological challenge.

Plasma-based technologies for DRM have been widely studied. [9-11] DRM can be performed using plasma technology without the use of precious metal catalysts. Activation of carbon dioxide and methane molecules can be achieved in different ways through plasma: by thermal decomposition, using stepwise vibrational excitation and electron collisions. For thermal plasma, thermal decomposition is the main process. In non-thermal plasma DRM, which is carried out at ambient temperatures, vibrational excitation is a more effective activation route.

The recent advances in DRM with plasma methods are summarized in several excellent reviews. [9-14] These indicate that DRM can be done with many plasma methods, giving conversions of around 40% at an energy cost range between 1.2-200 eV/molecule. Energy efficiencies of DRM performed through plasma technologies are difficult to determine, because during plasma driven DRM a variety of species and products are generated, including H_2, CO, CH_3•, H_2O, C_2H_2, C_2H_4, C_2H_5•, C_2H_6, C_3H_8 and C_4H_{10}. The wide product distribution affects the definition of energy efficiencies. Thus, plasma-based DRM processes are typically expressed in terms of *energy cost*, i.e., the amount of energy consumed by the DRM process in unit of eV/converted molecule. [11] The energy cost (eV/molecule $_{conv.}$) is therefore:

$$\frac{Power(kW) \times 60(s\ min^{-1}) \times 24.5(L\ mol^{-1}) \times 6.24 * 10^{21}(eV\ kJ^{-1})}{flowrate(L\ min^{-1}) \times \chi_{total} \times 6.022 * 10^{23}(molecule\ mol^{-1})} \quad (1)$$

Recently, several studies were published on DRM using Dielectric Barrier Discharges (DBD). [15-18] Good yields are reported, but only when a catalyst is inserted in the DBD reactor. The study by Ray et al. demonstrates that without catalyst DRM yields by plasma only are below 10%. Here we demonstrate much higher product yields without using a catalyst applying radio frequency inductively coupled plasma (RF-ICP). [19] RF-ICP has several advantages that makes it suitable for DRM:

1. RF allows to generate a non-thermal plasma at low pressures (i.e. 1 - 10^3 Pa). This is useful to drive the DRM process in a controlled way, without yielding a very wide variety of products.
2. RF plasma can be produced at low frequencies, ranging between 1 - 100 MHz. In this range, a large plasma volume of approximately the entire size of the plasma reactor can be generated. This ensures that the DRM process is driven in a fully homogeneous plasma. It is especially relevant for industry as it improves the scalability.
3. The RF plasma's energy efficiency can be optimized through an impedance matching network. By matching the impedance of the RF power generator to the RF plasma discharge one can minimize the reflected RF power to the plasma reactor.

Theoretically when an optimized coupling can be obtained between the plasma and the RF field, the energy efficiency of plasma-based selective heating can be up to 90%. [20-21]

[a] Dr. E. J. Devid, D. Zhang MSc., dr. D. Wang, dr. Q. Huang, Prof. dr. A. W. Kleyn
Center of Interface Dynamics for Sustainability
Institute of Materials, China Academy of Engineering Physics
596 Yinhe Road 7th section, Chengdu, Sichuan 610200, People's Republic of China
E-mail: ejdevid@outlook.com ; a.w.kleijn@contact.uva.nl

[b] D. Zhang MSc.
Leiden Institute of Chemistry
Leiden University
Einsteinweg 55, 2333 CC Leiden, The Netherlands

[c] M. Ronda-Lloret MSc., Prof. dr. G. Rothenberg, dr. N. Raveendran Shiju
Van 't Hoff Institute for Molecular Sciences
Faculty of Science, University of Amsterdam
P.O. Box 94157, 1090 GD Amsterdam, The Netherlands

[d] Dr. Q. Huang
School of Optoelectronic Engineering
Chongqing University of Posts and Telecommunication
Chongqing 400065, People's Republic of China

4. The electrodes for generating a RF-ICP are located outside the plasma reactor (see also experimental section). This is advantageous for the plasma-driven DRM process, as the non-thermal DRM plasma will not be contaminated by the metal electrodes.
5. Finally, RF-ICP allows to analyse the DRM process in a simple, accessible, non-invasive way, such as mass spectrometry, optical emission spectroscopy and laser-based methods.

Despite its potential, very little is reported on DRM by RF-ICP. Mozetic et al. published an extensive paper on activation of CH_4 by RF-ICP. [22] They showed that the main reactions products are -hydrocarbons, carbon deposits and H_2. The relative abundance of each product strongly depends on the plasma conditions. Increased energy deposition in the plasma leads to more hydrocarbon formation. Patino et al. also carried out studies on DRM with RF-ICP. The study focusses strongly on data analysis and experiment selection. [23] In addition they focussed on steam reforming, for which they get high syngas yields. However for DRM their yields are very low. Chen et al. studied the pyrolysis and oxidation of CH_4 in a He RF discharge. The authors complement their work with extensive kinetic modelling. [24] Other recent works have used radio frequency capacitively coupled plasma (RF-CCP). [25-30] These systems are similar to DBD. [11] The work with RF-CCP is more focused on dissociation of CH_4 and carbon deposition than on DRM. In CCP-based plasma setups the electrodes are inside the reaction vessel where the electrodes get quickly contaminated. External coils, as used in RF-ICP, are preferable for DRM.

Recently Ray et al. published in this Journal work on performing DRM in an improved DBD reactor with catalysts and the possibility of heating them up thermally to obtain higher yields of syngas. [19] Confirming earlier studies Ray et al. demonstrate that the energy cost of performing DRM by DBD both with or without catalysts remains very high (about 5 times the thermal equilibrium limit). [19] In our work we will compare the DRM performance of the improved plasma enhanced temperature DBD of Ray et al. with our plasma only RF-ICP reactor.

Another way to produce valuable hydrocarbons from methane without syngas involves the partial oxidation of methane to methanol. Using plasma technology also this route is available. [31-32]

Our work builds upon the work on methane activation by Mozetic et al. We utilize lower power, flow and pressure and discover that C2 compound formation decreases together with increased formation of H_2. This is a relevant finding for DRM. In addition, we show that DRM can be carried out in a RF-ICP setup with very high conversions, and can compete on energy cost with other types of plasma-driven DRM processes. Finally, we discuss the observation of water formation and its influence on hydrogen atom recycling in the process.

Results

QMS analysis of activation of pure CH_4

Quadrupole mass spectrometry (QMS) allows us to observe in real time both qualitatively and quantitativly the species formed in the plasma at low pressures. Details of the analysis are reported in the experimental section.

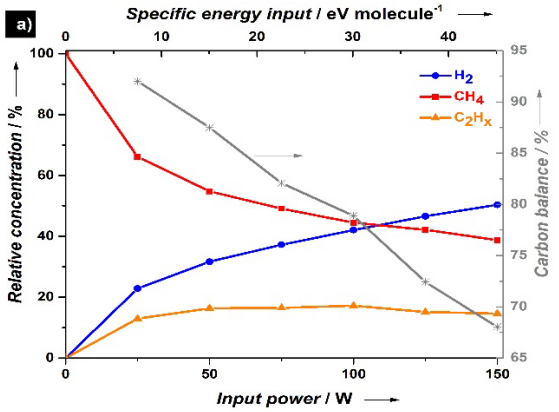

Figure 1a. Relative molecular concentration of effluent gas from pure CH_4 reforming at different input power. On the right y-axis is shown the carbon balance (%) where the ratio = ($CH_{4\,out}$ + 2 x $C_2H_{x\,out}$) / ($CH_{4\,in}$) x 100 %. Reaction conditions: Feed: CH_4; Flow: 50 sccm; Pressure: 44 Pa

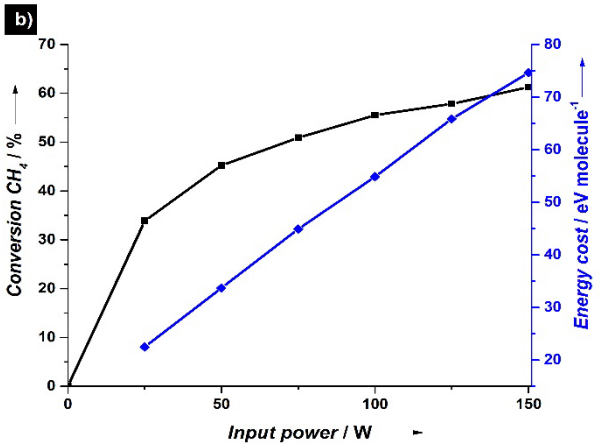

Figure 1b. Conversion of CH_4 as function of input power. The energy cost for pure CH_4 reforming by RF-ICP is plotted on the right (blue coloured) Y-axis. The energy cost is defined as power (kW) *60 (s/min.) * 24.5 (L/mol) * 6.24 *10^{21} (eV/kJ) divided by (flowrate (L/min.) * χ_{Total} * 6.022 * 10^{23} (molecule/mol)). The reaction conditions: Feed: CH_4; Flow: 50 sccm; Pressure: 44 Pa

Figure 1a shows the relative concentrations of product species from pure CH_4 reforming in RF-ICP and the carbon balance at different input power. For decomposition of pure CH_4, the product's H/C ratio should be 4 (irrespectively of the RF power). In fact, this ratio increases from 4 at 0 W to 4.6 at 150 W. This indicates a loss of carbon by deposition of a carbonaceous film on the reactor wall. From the carbon balance plotted in Figure 1a (calculated as given in the caption and following ref 19) is shown that with increasing power the loss of carbon behaves linearly. With increasing specific energy input more CH_4 dissociates into H_2 and C where the carbon gets deposited at the reactor walls.

A direct *in situ* spectroscopic analysis of this film is not possible. However, we see the formation of a yellow film inside the reactor tube after prolonged operation. Elsewhere, we measured the electron temperature. In the present arrangement this was not possible. [20, 33] However, based upon our results we estimate it to be between 2 and 5 eV. This means that direct electronic excitation of CO_2 is unlikely.

Our results show that RF-ICP can effectively activate methane molecules. The main products of CH_4 reforming were hydrogen

and C2 hydrocarbons. Increasing the power, the conversion of methane increased up to 60% (see Figure 1a and 1b). The yields of H_2 and C2 hydrocarbons sharply increased below 50 W. With further increase in power, H_2 yield increased steadily and C2 yield stabilized. The highest concentration was for H_2 with 50% (at 150 W) of all gaseous products (Figure 1a) and the total H_2 yield over H-containing products was 35% at 150 W. The energy cost for CH_4 reforming follows here a linear trend as function of the input power, which is lower compared to most plasma-based DRM studies done in DBD reactors. [11, 19] Thus, RF-ICP is more energy efficient than DBD for CH_4 reforming.

Previously, we could not determine which fraction of the RF power is absorbed by the plasma. [20] In the case of RF plasma etchers the energy efficiency can be up to 90%. [21] Therefore, our numbers for energy input into the plasma should not be seen as the ultimate obtainable by RF. Assuming that the RF power emitted into the coil is entirely absorbed by the plasma, we can determine the specific energy input (SEI) into the CH_4. The corresponding SEI is given on the top axis of Figure 1a. A power of 150 W corresponds to a SEI of 46 eV/CH_4. The corresponding energy efficiency depends on the specific reaction. The heat of formation of CH_4 from C(solid) and H_2 is 0.77 eV. The heats of formation of C_2H_x vary from 2.36 to –0.87 eV/molecule.

We also studied the pressure dependence of the methane conversion at a power of 150 W and pressures from 50 to 200 Pa at the same flow of 50 sccm (data not shown). We observe that the conversion of CH_4 decreases with increasing pressure. This is a factor of 1.5 over the pressure range mentioned.

QMS analysis of activation of mixtures of CH_4 and CO_2

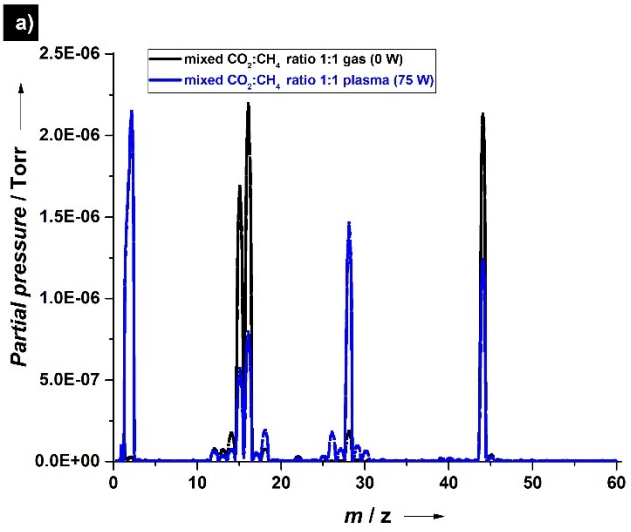

Figure 2a. Mass spectra of real time observed mixed CO_2:CH_4 (1:1) gas effluent at 0 W (see black line) versus the same mixed CO_2:CH_4 (1:1) gas now turned into plasma (see blue line). Reaction conditions: Total feed is 50 sccm; input power: 75 W; Pressure mixed CO_2:CH_4 (1:1) gas effluent at 0 W is 36 Pa. Pressure mixed CO_2:CH_4 (1:1) plasma effluent at 75 W is 40 Pa.

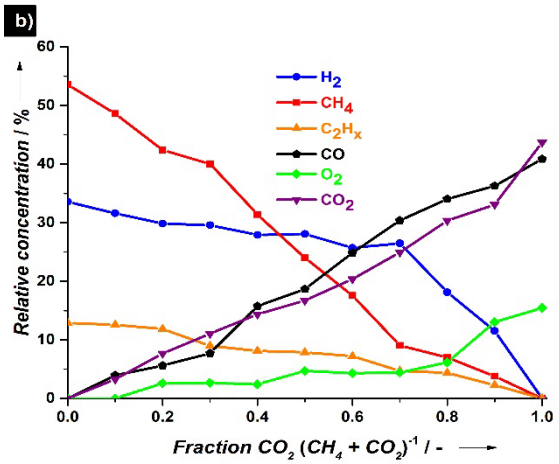

Figure 2b. Relative molecular concentrations of effluent gas from mixed CH_4/CO_2 reforming at different CO_2/(CH_4+CO_2) fractions. Reaction conditions: Feed: CH_4 and (or) CO_2; input power: 75 W; Total flow: 50 sccm; Pressure 50 Pa.

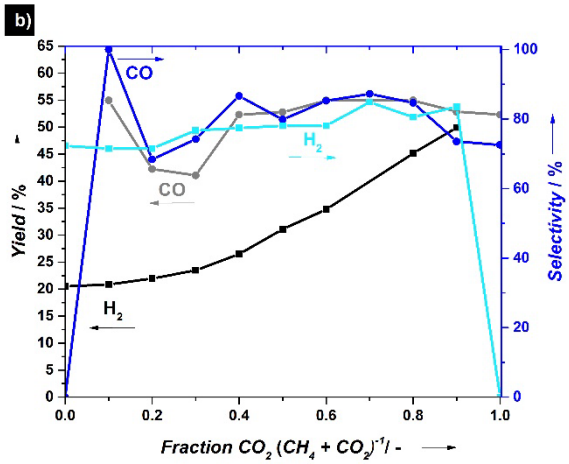

Figure 2c. H_2 and CO yields as function of the fraction CO_2/(CH_4+CO_2). The H_2 yield is defined as 2 * H_2 intensity divided by the total H intensity detected in the products (H_2+CH_4+C_2H_x). The CO yield is defined as the CO intensity over the sum of CO and CO_2 intensities. The H_2 selectivity is defined as the H_2 intensity divided by the sum of the products (H_2+C_2H_x) intensities converted from CH_4. The CO selectivity is defined as the CO intensity divided by the sum of the products (CO+O_2) intensities converted from CO_2. Reaction conditions: Feed: CH_4 and (or) CO_2; input power: 75 W; Total flow: 50 sccm; Pressure 50 Pa.

The DRM process is activated through a non-thermal plasma generated by RF-ICP (see also the Experimental section). QMS allows us to real time probe in a non-evasive way both qualitative and quantitative the low-pressure effluent gases from our plasma reactor. Figure 2a shows the observed unreacted reactants (see black line on mass spectrum) and the formed species during plasma driven DRM at 75 W (see blue line). Figure 2a shows clearly that CH_4 and CO_2 are converted by plasma only into H_2 and CO. In order to extract quantitative information from QMS, a calibration is performed for each gas species (such as H_2, CO, CH_4, CO_2, O_2) that requires to be identified in the plasma reactor. The calibration and analysis are described in the experimental section.

The feed fraction of CO_2/(CH_4+CO_2) is one of the key factors affecting the dry reforming of methane. [10, 34-36] Figure 2b shows the relative molecular concentrations derived from QMS signals of effluent gas from mixed CH_4/CO_2 reforming in RF-ICP at

different $CO_2/(CH_4+CO_2)$ fractions. Detection of H_2O is difficult, because it is efficiently absorbed by the system walls. This is confirmed by the observation that it can take more than one hour to bring the H_2O level in the residual gas back to a low level of a few Pa. For the C_2H_x contribution, we use the same method described previously for the pure CH_4 feed.

To test the data consistency we analysed the H/C and O/C ratios. For a 1:1 mixture of CH_4 and CO_2 about 20% of the C-atoms are 'missing', which indicates that they are probably deposited on the system walls. In the case of a CO_2 rich plasma O/C below the expected value of 2 by up to 30%. We infer that both C and O can be adsorbed by the walls of the pumping system and potentially lead to H_2O, via the presence of H, that also can be absorbed on the system walls and escape detection.

As shown in Figure 2b, the main products of the dry reforming of methane in RF-ICP are H_2, CO, O_2 and C2 hydrocarbons. Changing the ratio of CO_2:CH_4 significantly alters the ratio of the products. Increasing the proportion of CO_2 from 0% to 70%, the C2 hydrocarbons decrease, while the H_2 concentration remains almost same (Figure 2b). In plasma, pure CO_2 is decomposed into CO and O_2. For pure CO_2 the O_2 relative concentration (17%) is almost 50% of that of the CO concentration (40%). With a small amount of CH_4 (0.8 $CO_2/(CH_4+CO_2)$) added, the O_2 decreased from 17% (at 100% CO_2 feed) to 7%. This is attributed to the rapid reaction of CH_4 with O to produce H_2O or OH, both of which are not detected by QMS. In addition, the O_2 varies slightly between experiments with low $CO_2/(CH_4+CO_2)$ fractions. Most likely it depends on the amount of H_2O adsorption on the system walls.

The yields and selectivity of H_2 and CO are plotted in Figure 2c. The H_2 yield with respect to the incident H-atoms (in CH_4) is increasing with the CO_2 content in the flow. The CO yield is basically constant between 40% and 55% at the $CO_2/(CH_4+CO_2)$ feed fractions 0.4-0.9. The reason for the appearance of a dip in the CO yield around 0.2 and 0.3 feed ratio is not known. The selectivity of H_2 increases from 72.3% to 83.5% when the fraction $CO_2/(CH_4+CO_2)$ reaches unity.

The selectivity of CO peaks to 100% at the fraction 0.1. Beyond the fraction 0.1 the selectivity shows small fluctuations around 80%. Higher fractions $CO_2/(CH_4+CO_2)$ show that the presence of more CO_2 in the mix enable the increasing selectivity and yield of H_2. The decrease of the CH_4 in the mix shows that the decomposition of CH_4 affects little to non the selectivity and yield of CO.

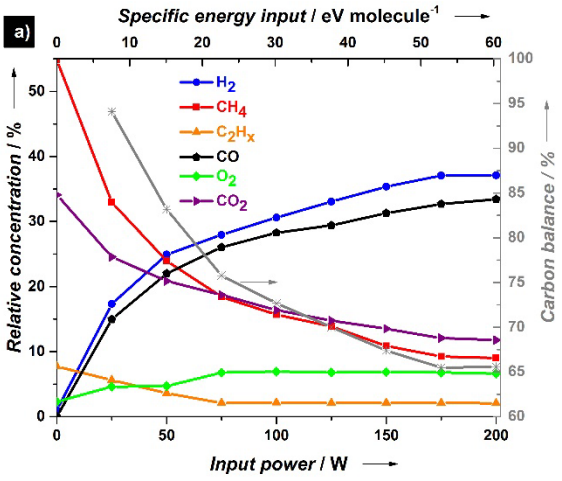

Figure 3a. Relative molecular concentrations of effluent gas from CH_4 and CO_2 reforming at a fixed CH_4 /CO_2 ratio of unity as a function of input power. The right ordinate shows the carbon balance (%) where the ratio = $(CH_{4\ out} + CO_{2\ out} + 2 \times C_2H_{x\ out}) / (CH_{4\ in} + CO_{2\ in}) \times 100$ %. Reaction conditions: Equal feed ratio CH_4 and CO_2; Total flow: 50 sccm.

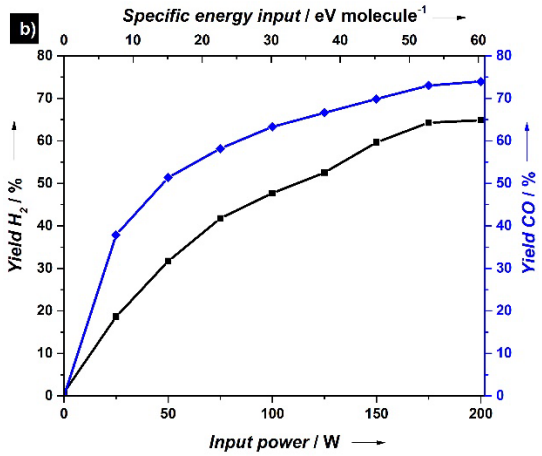

Figure 3b. The H_2 and CO yields as function of input power and SEI. Reaction conditions: Equal feed ratio CH_4 and CO_2; Total flow: 50 sccm.

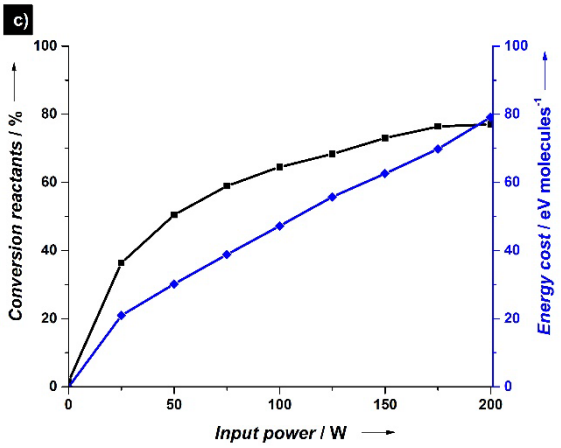

Figure 3c. Total conversion of reactants and the energy costs of effluent gas from mixed CH_4/CO_2 reforming at a fixed CH_4/CO_2 ratio of unity as a function of input power. Reaction conditions: Equal feed ratio CH_4 and CO_2; Total flow: 50 sccm.

Figure 3a shows the power dependence of the relative concentrations derived from QMS signals of the effluent gas from mixed CH_4/CO_2 reforming in RF-ICP at CH_4/CO_2=1. Figure 3a also shows the carbon balance of the mixed CH_4/CO_2 reforming in RF-ICP at CH_4/CO_2=1. With increasing specific energy input the decrease of carbon balance behaves non-linearly. At higher input powers a steady state is reached in carbon loss. The presence of a CO_2 feed at CH_4/CO_2=1 enables to limit the carbon loss. Presumably the carbon from the dissociated CH_4 reacts with the atomic O atoms from the dissociated CO_2. This observation corresponds with the steady state concentration of O_2 in Figure 3a that explains why the O_2 concentration is not increasing further with increasing power beyond 75 W.

RF-ICP grants here the combination of carbon and atomic oxygen into CO thereby increasing further the yield of CO compared to the yield of C_2H_X molecules.

Measurement conditions are similar to those previously discussed about Figure 2. The H/C and O/C ratios were analysed to test the consistency of the data. For a 1:1 mixture of CH_4 and CO_2 about 20% C-atoms is 'missing' irrespective of power. The O/C ratio can deviate from the ideal value 1 by more than 20%. Formation of H_2O is likely under these conditions.

The yields of H_2 and CO are plotted in Figure 3b. Both H_2 and CO yields gradually increase with increasing power. At 200 W, H_2 yield is 65% and CO yield is 74%.

The total conversion of mixed CH_4/CO_2 (1:1) reaches 77% (200 W) by plasma only RF-ICP (see Figure 3c). This value is better than the absolute conversion of CH_4 and CO_2 of Ray et al. respectively 68% and 65% obtained in their plasma-assisted thermal DBD reactor with addition of their best performing catalyst 15% Ni/Al_2O_3. [19] Without catalyst Ray et al. obtain a maximum yield for both CO ad H_2 of 10%. In this case power and flow are lower so that a good comparison cannot be made. DRM driven by RF-ICP plasma only has the advantage that no catalysts are required to obtain high syngas yields, and so there is no need to find suitable catalysts resistant to coke formation.

Figure 3c shows that the energy cost of the dry reforming of methane at a CO_2:CH_4 ratio of 1:1 is here lower than the energy cost of reforming CH_4 only (see Figure 1b). RF-ICP on CO_2:CH_4 mixed ratios provides energy costs comparable to DRM studies done by atmospheric pressure glow discharge (APGD) (see table 1). [11]

Table 1 shows the total conversion and energy cost for multiple different plasma driven DRM processes (originating from ref [11]). Our RF-ICP plasma driven DRM process reaches a total conversion range of 0 - 77% (from 0 W till 200 W) and an energy cost range of 0 - 79 eV/molecule (from 0 W till 200 W). Comparing our performance ranges with the ones from table 1, we observe that our RF-ICP driven DRM outperform microwave (MW) and DBD operated DRM processes. The DRM processes operated by DBD [37-39] reach close the total conversion and energy cost of our RF-ICP driven DRM performances.

Furthermore our RF-ICP driven DRM performances reach closely the performances of APGD [40-41] .

Finally, RF-ICP driven DRM reaches total conversions similar to corona and spark driven DRM. But the energy cost with our RF-ICP is respectively about a factor 2 and factor 5 higher. However, we note that the efficiency of our RF-ICP system is not optimized and that better efficiencies should be obtainable using RF-ICP. By tuning the mixed ratios of the reactants, the energy cost of DRM by RF-ICP can be further changed and optimized.

Table 1. Total conversion versus energy cost of DRM process by different plasma systems [11, 37-44]

	Gliding Arc	Atmospheric Pressure Glow Discharges	Spark	Nanosecond pulse discharge	Corona discharge	MW	DBD
Total conversion (%)	3-44	36-88	7.5-96	0-64	14-90	50-73	0-85
Energy cost (eV/ molecule)	1-50	0.9-60	3.2-10.6	3-100	4.2-30	120-400	12-600

OES analysis of activation of mixtures of CH_4 and CO_2

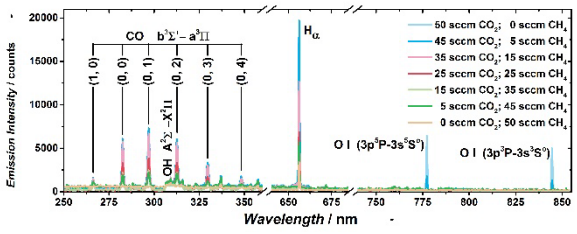

Figure 4. Optical emission spectra from CO_2 and CH_4 reforming at different CH_4/CO_2 ratio. Reaction conditions: Feed: CH_4 and (or) CO_2; Input power: 75 W; Total flow: 50 sccm; Pressure 50 Pa.

We measured the optical emission spectra (OES) for CH_4/CO_2 mixtures as a function of composition (Figure 4) and as a function of input power for an equimolar mixture. In the analysis we focus on the emission of the CO b$^3\Sigma^+$ state, OH, O-atoms and H-atoms. To compare the emission intensity at different composition of the mixture, the peaks of H_α and 0-0, 0-1 transition of CO (b$^3\Sigma^+$ - a$^3\Pi$) system are integrated (see Figure 5).

Figures 4 and 6 show CO vibrational progressions that do not exhibit large vibrational excitation, such as the ones we previously observed for CO_2 plasma diluted by Ar. [20] The CO emission spectrum changes when tuning the CH_4/CO_2 ratios (see Figure 4). The emission from CO and O atoms will dominate the optical emission spectra under a pure CO_2 feed. As the proportion of CH_4 in the feed is increased from 0% to 10%, the emission peak of O atoms decreased drastically, and an OH emission band ($A^2\Sigma^+$ - $X^2\Pi$) appears in the 300 nm-320 nm region. Besides emission from OH also a large H_α emission intensity was observed at 10% CH_4 in the mixed feed CH_4/CO_2 case rather than in pure CH_4 which has highest H/C ratio and H_2 yields.

The integrated intensity of two CO lines, two O-atom lines and H_α emission are plotted in Figure 5 as a function of the relative CO_2 content of the feed. The CO emission shows a linear increase with CO_2 content, very similar to the CO yield observed by QMS, cf. Figure 2b. The linear increase seen in both QMS and OES of the CO signal confirms that the decomposition of the mass 28 signal to C_2H_x and CO is done correctly. The QMS data shows no leveling off of the CO signal as seen for CO emission in Figure 5. We attribute this to change in plasma parameters at the highest CO_2 fraction, leading to a smaller electronic excitation of CO.

The O-atom signal in Figure 5 shows a marked increase at the highest CO_2 content (> 0.7). The H_α emission shows a peak at the CO_2 content of 0.9, where the number of H-atoms i ntroduced by CH_4 is already very low.

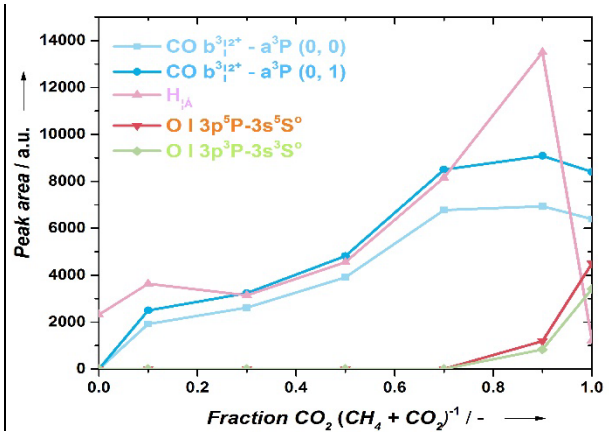

Figure 5. Integrated emission intensity of 0-0, 0-1 transition of CO ($b^3\Sigma^+$ - $a^3\Pi$) system, H_α and O I ($3p^5P \rightarrow 3s^5S^\circ$, $3p^3P \rightarrow 3s^3S^\circ$). Reaction conditions: Input power 75 W; Total flow: 50 sccm; Pressure: 50 Pa

The power dependence of the OES is shown in Figures 6a and 6b where the same spectral regions are shown as in Figure 4. We see that the emission of H_α and 0-0, 0-1 transition of CO ($b^3\Sigma^+$ - $a^3\Pi$) system increase as the power is increasing. For equimolar mixtures no O-atom emission is observed. Additionally, the CO_2^+ doublet is observed, centered at λ=288.3 nm and λ=289.6 nm. OH emission is also observed (especially at higher power) for the equimolar mixture. The line integrated intensities are shown in Figure 7. The trends observed are very similar to what is observed by the QMS intensities in Figure 3.

Figure 6b shows that the emission of H_α during RF-ICP driven DRM intensifies by increasing the power to 75 W. Above 75 W, emission of H_α levels off as function of the input power. This indicates that RF-ICP driven DRM enables easy excitation of hydrogen into H_α. RF-ICP offers an easy and accessible way to yield high levels of H_α.

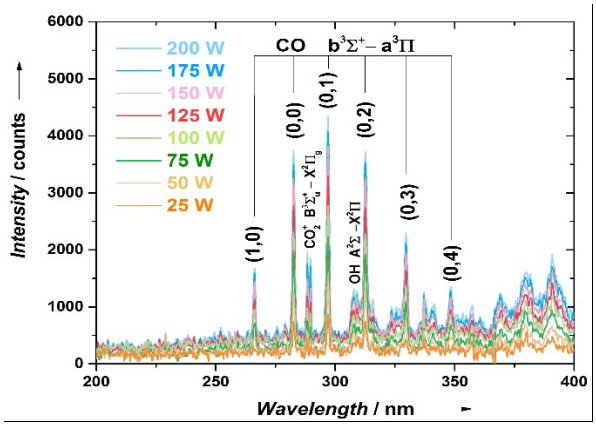

Figure 6a. Optical emission spectra from CO_2 and CH_4 reforming in RF-ICP at different input power in two spectral ranges. Reaction conditions: Feed: 25 sccm CH_4, 25 sccm CO_2; Pressure: 39 Pa.

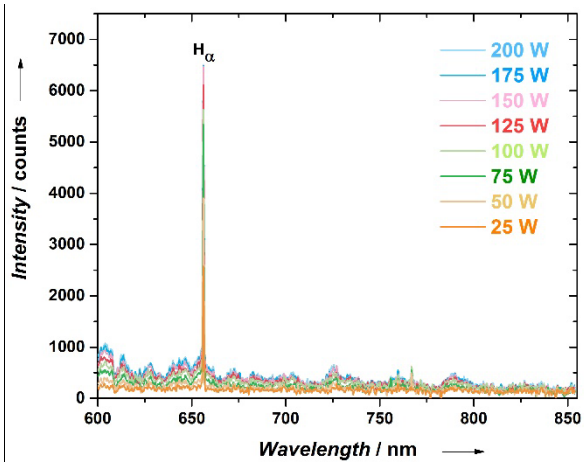

Figure 6b. Optical emission spectra from mixed CH_4/CO_2 reforming in RF-ICP at different input power in two spectral ranges. Reaction conditions: Feed: 25 sccm CH_4, 25 sccm CO_2; Pressure 39 Pa.

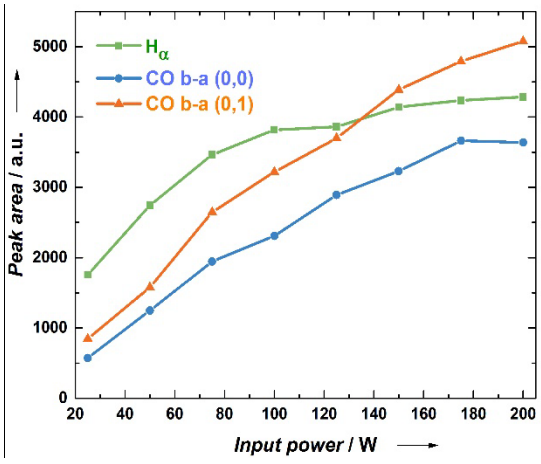

Figure 7. Integrated emission intensity of 0-0, 0-1 transition of CO ($b^3\Sigma^+$ - $a^3\Pi$) system and H_α as function of input power. Reaction conditions: Feed: 25 sccm CH_4, 25 sccm CO_2; Pressure 39 Pa.

Discussion

Activation of methane

For a comparison to our DRM experiments, we carried out RF-ICP induced activation of pure methane. With increasing SEI we observed an increasing dissociation. At the highest power (150 W, SEI = 45.71 eV/molecule), 60% of CH_4 was converted into H_2, C_2H_x and C deposit. Conversion efficiencies of CH_4 are very significant at these power levels. There are very few similar studies using RF-ICP. The most comparable work is the study by Mozetic et al [22] These authors also studied pure CH_4 discharges. However, their setup is different, as it contains a special after-glow chamber connected to the plasma chamber via a small orifice. Moreover, the RF power used in their study (ca. 1200 W) is six times higher than what we use here. Our system gives higher conversion, which can be attributed to the lower operating pressure and possibly the absence of a buffer chamber. Comparing our results with those of Mozetic et al., we conclude that methane conversion of more than 50% can be obtained at lower power levels and pressures as well. This indicates that efficient DRM can be expected with RF-ICP, as we discuss below.

Activation of mixtures of CH_4 and CO_2

The product concentration of a CH_4/CO_2 mixture is shown in Figure 2b as function of the CO_2:CH_4 feed composition. As expected, the CH_4 signal linearly decreases with the $CO_2/(CH_4+CO_2)$ fraction, whereas the CO_2 relative concentration linearly increases. Also, the CO concentration linearly increases. The CO yield is constant at 48% at 75 W. Figure 2c shows that the CO yield is nearly constant as function of feed composition. This implies that the conversion of CO_2 into CO is independent of feed composition. Figure 3b shows that the CO yield increases with power, where even values of 75% CO yield can be reached at 200 W. The CO yield in DRM at 200 W is higher than we measured for pure CO_2. The limited yield in pure CO_2 plasma is attributed to recombination of the reaction products CO+O back to the reactant CO_2, see e.g. [45-47]. RF-ICP driven DRM enables the suppression of the reverse reaction.

The product H_2 in Figure 2b is not proportional to the fraction of CH_4 in the feed. It is almost constant at a level 27-33% and drops at $CO_2/(CH_4+CO_2)$ fractions above 0.7. As a consequence, the H_2 yield (see Figure 2c) is increasing as a function of $CO_2/(CH_4+CO_2)$ fraction. Increasing power, as shown in Figure 3b, increased the H_2 yield to almost 75%. This shows that the formation of syngas has a high probability. Thus, RF-ICP driven DRM is an efficient and clean way to produce syngas. The energy cost between CH_4 reforming (see Figure 1b) versus mixed CO_2:CH_4 reforming (see Figure 3c) shows significant differences, especially when compared with the total conversion. RF-ICP reforming of mixed CO_2:CH_4 ratios achieves lower energy costs while significantly increasing both H_2 and CO yields at low powers (see Figure 3b). Optimizing the coupling of power into the plasma will be a next step in this work to further enhance the energy efficiency.

The CO optical emission intensity shows a similar trend with QMS regarding the mass 28 peak. This indicates that most of the product under CO_2 feed is CO. Additionally, the H_2 yield is very high. This indicates that syngas can be produced by DRM through RF-ICP at low specific energy.

H_α emission

A most remarkable observation in OES is the strong H_α emission at high $CO_2/(CH_4+CO_2)$ fractions in the feed, as shown in Figures 4 and 5. The highest optical emission intensity of H_α was achieved at 90% CO_2 in the feed, where relatively few H-atoms are introduced into the discharge. Nevertheless, the strong H_α emission indicates that a high number of H-atoms is present in the plasma. We attribute this signal to the presence of H_2O in the discharge, preferably for a high CO_2 content. H_2O cannot be easily detected in the discharge by QMS, but its presence is here deduced from the optical emission of OH (see Figure 6). We believe that this is due to electron impact driven dissociation of H_2O. The H and OH emissions are not equally strong due to different spectral properties. The process leading to strong H_α emission is similar to that observed before by Mucha et al. for diamond forming CH_4 discharges. [48]

Conclusions

Our work demonstrates that RF-ICP discharges can form syngas by dry reforming of methane (DRM). Syngas yields of more than 70% were observed above 150 W at an equal feed CH_4/CO_2 ratio. Moreover, RF-ICP driven reforming of mixed CO_2:CH_4 ratios demonstrates low energy costs comparable with APGD driven DRM and much lower than DBD driven DRM. By controlling the mixing ratios of CO_2:CH_4 we can tune up the yield of H_2 while minimizing the formation C2 compounds. At high $CO_2/(CH_4+CO_2)$ fractions in the feed, we observe significant amounts of H_α. The presence of H_α and OH in a RF-ICP driven DRM process suppresses the recombination of CO+O, as the CO yields in DRM keep exceeding the CO yields found during RF-ICP driven discharge of pure CO_2. The formation of water plays a key role in the hydrogen atom recycling in a RF-ICP driven DRM process. All in all, we show that the dry reforming of methane using radio frequency inductively coupled plasma is a promising alternative for transforming the greenhouse gases methane and CO_2 to valuable syngas under moderate conditions.

Experimental Section

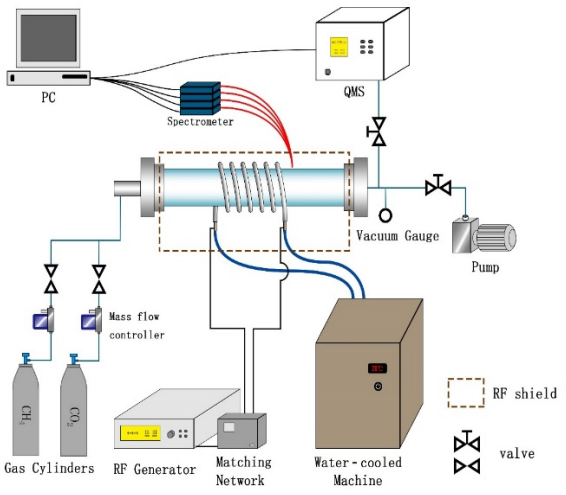

Figure 8. Schematic diagram of experimental setup.

All experiments were carried out in a designated RF-ICP reactor constructed in-house (Figure 8). The plasma reactor consists of a quartz tube, with a diameter of 40 mm and length of 600 mm. It is supported by two stainless steel flanges and sealed by O-rings. The reactor tube is surrounded by a water-cooled copper coil. To establish efficient coupling of RF energy into the plasma, a matching box is kept between the RF power supply (13.56 MHz, 2 kW) and the copper coil. In contrast to our previous experiments we could not mount a Langmuir probe to measure plasma parameters. A detailed technical description of the setup is published elsewhere. [20, 49-50]

The maximum power used was 350 W and the reflected power was kept under 1 W by the matching box. However, this does not imply that all power from the supply is coupled into the plasma. Ohmic losses and RF losses by radiation will decrease the power actually coupled into the plasma. We have not optimized the coupling of power into the plasma and only note that earlier work shows that very high coupling can be achieved.

The gases used in the reaction were directly obtained from gas cylinders and mixed before going into the reactor. Each gas cylinder was equipped with calibrated mass flow controllers (MFC, Sevenstar D07-19B) to set the flow. The plasma ignited inside the reactor tube, after supplying RF power. Prior to feeding the reaction gases, the reactor was evacuated to 1 Pa by a rotary pump with the nominal pumping speed around 18 L/s.

The light emitted by the plasma was collected by an optical fiber located 1.5 cm downstream from the coil, viewing the center of the reactor tube. The data was transmitted to our UV-VIS-NIR spectrometers (spectrometer, StellarNet LSR-NIR3b, LSR-UV2, LSR-VIS4b and LSR-VIS4). Data was analyzed as described earlier. [20]

To study the effect of the specific RF-ICP power supply and pressure on DRM, the experiments were carried out in different modes. Firstly, at various power levels (from 0 W to 150 W), while the CH_4 or CO_2 flow were fixed at 50 standard cubic centimeter per minute (herein: sccm). Secondly, the power was kept constant at 75 W and the pressure was changed from 50 Pa to 300 Pa at a total flow of 50 sccm. Thirdly, we studied the effect of the feed gas composition. For that we modified the fraction $CO_2/(CH_4+CO_2)$ while keeping the total feed gas rate and the power constant.

The composition of the gaseous products from the plasma reactor was determined by quadrupole mass spectrometry (QMS). This is a powerful tool, because the gas composition can be measured in real time. In this way the stability of the plasma can be checked continuously. Analysing the mass spectra can be tricky, as different components lead to ions with the same mass such as 28, and the sensitivity for each species can differ. Moreover, the transmission of the instrument may be mass dependent. To solve this, we used a simple approach to obtain the composition of the effluent gas. We determined the relative yields of equimolar mixtures of H_2, CH_4, CO, O_2 or CO_2 and Ar by QMS. The ratio of the yield of the parent molecular ions concerned and Ar^+, was used to determine the relative efficiency for each gas. This analysis yields the relative composition of the product gas as a function of one of the experimental variables.

To deconvolute the contributions to for instance the mass 28 peak, we performed an interpolation between extreme cases, where the composition is known, such as experiments with pure CO_2 or CH_4. In this interpolation we took the height of secondary peaks into consideration. The interpolation was done by hand on the basis of individual mass spectra. Intensities of C_2H_x species are hard to determine individually, also because of overlapping peaks in the mass spectrum. We got the C_2H_x signal by adding the intensities of the dominant peaks.QMS has internal consistency checks, namely the H/C and O/C ratio of the measured intensities. The ratio is set by the reactant flow, and cannot be changed by plasma action. For pure CH_4: H/C=4 and for pure CO_2: O/C=2. We checked that the analysis is done in a consistent way.

Previously, we reported the analysis data for the decomposition of pure CH_4 and pure CO_2 in this RF-ICP reactor setup. [20, 49] Those studies form the basis for the current work, which focuses on pure methane and mixed CH_4/CO_2 reforming. Our calibration method is similar to the method described by Nguyen et al., where a fixed flow of argon flows into the plasma reactor with a varying flow of the targeted gas species. [51] From the ratios of the partial pressure of Argon and the targeted gas species together with the flow ratios of each gases, a calibration factor can be determined. With the calibration factor (i.e. the slope of the line) the ratio of partial pressures can now be plotted with the ratio of the flow rates of the gases for H_2, CO, CH_4, CO_2, O_2. This linear extrapolation together with the extrapolation from data between steady state gases that was activated by plasma (input power > 0) versus not activated by plasma (input power is 0 W) allows us to determine the contribution to the mass 16 and mass 28 signals. From limiting cases, the composition of both mass 16 and mass 28 is then known and we can make distinction between the ions O^+ versus CH_4^+ and $C_2H_4^+$ versus CO^+.
Further the fragmentation pattern and fragmentation ratio of gas species like CH_4 and CO_2 are taken into account by a preliminary background scan. By taking a QMS background scan of CO_2 we identify and check the fragmentation pattern and ratio of CO_2. This enable us to check and correct the mass spectra on the amount of CO that originate from the fragmentation of the parent molecule CO_2 in the ionizer of the QMS.

The reproducibility of experimental runs was better than 20%. Within a single run, the signals for individual mass peaks reproduce to within 10% after stabilization of the system for a few minutes. The relative intensity of molecular C_2H_2, C_2H_4, and C_2H_6 cannot easily be derived from mass spectrometry. [22, 52-53] Since this decomposition is not relevant for the present study, we added the various contributions and give a total signal of C_2H_x. The various molecules have different ionization cross sections, so we expect that there can be systematic errors up to 20% for the C_2H_x signal.

Acknowledgements

This work has the support of the National Natural Science Foundation of China (Grant No. 51561135013 and 21603202). We thank the Netherlands Scientific Organisation (NWO) for the grant “Developing novel catalytic materials for converting CO_2, methane and ethane to high-value chemicals in a hybrid plasma-catalytic reactor” (China.15.119).

Keywords: radio frequency inductively coupled plasma • dry reforming of methane • quadrupole mass spectrometry • optical emission spectroscopy • syngas

[1] T. L. Frolicher, E. M. Fischer, N. Gruber, *Nature* **2018**, *560*, 360.
[2] J. D. Shakun, P. U. Clark, F. He, S. A. Marcott, A. C. Mix, Z. Y. Liu, B. Otto-Bliesner, A. Schmittner, E. Bard, *Nature* **2012**, *484*, 49.
[3] J. R. Malcolm, C. R. Liu, R. P. Neilson, L. Hansen, L. Hannah, *Conserv. Biol.* **2006**, *20*, 538.
[4] D. Hone, *Sky: Meeting the goals of the Paris agreement*, Shell International B.V., https://www.shell.com/energy-and-innovation/the-energy-future/scenarios/shell-scenario-sky.html, **2018**.
[5] O. R. Inderwildi, S. J. Jenkins, D. A. King, *J. Phys. Chem. C* **2008**, *112*, 1305.
[6] D. Pakhare, J. Spivey, *Chem. Soc. Rev.* **2014**, *43*, 7813.
[7] J. L. Ewbank, L. Kovarik, C. C. Kenvin, C. Sievers, *Green Chem.* **2014**, *16*, 885.
[8] T. Stroud, T. J. Smith, E. Le Sache, J. L. Santos, M. A. Centeno, H. Arellano-Garcia, J. A. Odriozola, T. R. Reina, *Appl. Catal. B-Environ.* **2018**, *224*, 125.
[9] X. M. Tao, M. G. Bai, X. A. Li, H. L. Long, S. Y. Shang, Y. X. Yin, X. Y. Dai, *Prog. Energy Combust. Sci.* **2011**, *37*, 113.
[10] W. C. Chung, M. B. Chang, *Renew. Sust. Energ. Rev.* **2016**, *62*, 13.
[11] R. Snoeckx, A. Bogaerts, *Chem. Soc. Rev.* **2017**, *46*, 5805.
[12] A. H. Khoja, M. Tahir, N. A. S. Amin, *Energy Conv. Manag.* **2019**, *183*, 529.

[13] X. Tu, J. C. Whitehead, *Appl. Catal. B-Environ.* **2012**, *125*, 439.
[14] S. Ravasio, C. Cavallotti, *Chem. Eng. Sci.* **2012**, *84*, 580.
[15] A. H. Khoja, M. Tahir, N. A. S. Amin, *International Journal of Hydrogen Energy* **2019**, *44*, 11774.
[16] A. H. Khoja, M. Tahir, N. A. S. Amin, *Energy Conv. Manag.* **2017**, *144*, 262.
[17] S. Kameshima, K. Tamura, Y. Ishibashi, T. Nozaki, *Catal. Today* **2015**, *256*, 67.
[18] Y. X. Zeng, L. Wang, C. F. Wu, J. Q. Wang, B. X. Shen, X. Tu, *Appl. Catal. B-Environ.* **2018**, *224*, 469.
[19] D. Ray, D. Nepak, S. Janampelli, P. Goshal, C. Subrahmanyam, *Energy Technol.* **2019**, *7*, 11.
[20] D. Y. Zhang, Q. Huang, E. J. Devid, E. Schuler, N. R. Shiju, G. Rothenberg, G. van Rooij, R. L. Yang, K. Z. Liu, A. W. Kleyn, *J. Phys. Chem. C* **2018**, *122*, 19338.
[21] R. B. Piejak, V. A. Godyak, B. M. Alexandrovich, *Plasma Sources Science & Technology* **1992**, *1*, 179.
[22] M. Mozetic, A. Vesel, D. Alegre, F. L. Tabares, *J. Appl. Phys.* **2011**, *110*, 10.
[23] P. Patino, Y. Perez, M. Caetano, *Fuel* **2005**, *84*, 2008.
[24] Q. Chen, X. F. Yang, J. T. Sun, X. J. Zhang, X. G. Mao, Y. G. Ju, B. E. Koel, *Plasma Chemistry and Plasma Processing* **2017**, *37*, 1551.
[25] C. H. Tsai, T. H. Hsieh, *Ind. Eng. Chem. Res.* **2004**, *43*, 4043.
[26] K. Katayama, S. Fukada, M. Nishikawa, *Fusion Engrg. Des.* **2010**, *85*, 1381.
[27] B. Jeon, E. D. Park, Y. K. Kim, *Res. Chem. Intermed.* **2018**, *44*, 3761.
[28] F. I. Bohrer, C. N. Colesniuc, J. Park, M. E. Ruidiaz, I. K. Schuller, A. C. Kummel, W. C. Trogler, *J. Am. Chem. Soc.* **2009**, *131*, 478.
[29] C. S. Shen, D. K. Sun, H. S. Yang, *J. Nat. Gas Chem.* **2011**, *20*, 449.
[30] Q. Chen, J. T. Sun, X. J. Zhang, *Chin. J. Chem. Eng.* **2018**, *26*, 1041.
[31] P. Chawdhury, D. Ray, D. Nepak, C. Subrahmanyam, *Journal of Physics D-Applied Physics* **2019**, *52*, 11.
[32] L. Wang, Y. H. Yi, C. F. Wu, H. C. Guo, X. Tu, *Angew. Chem.-Int. Edit.* **2017**, *56*, 13679.
[33] H. Singh, D. B. Graves, *J. Appl. Phys.* **2000**, *88*, 3889.
[34] D. H. Li, X. Li, M. G. Bai, X. M. Tao, S. Y. Shang, X. Y. Dai, Y. X. Yin, *International Journal of Hydrogen Energy* **2009**, *34*, 308.
[35] Y. Xu, Q. Wei, H. L. Long, X. Q. Zhang, S. Y. Shang, X. Y. Dai, Y. X. Yin, *International Journal of Hydrogen Energy* **2013**, *38*, 1384.
[36] H. L. Long, S. Y. Shang, X. M. Tao, Y. P. Yin, X. Y. Dai, *International Journal of Hydrogen Energy* **2008**, *33*, 5510.
[37] R. Snoeckx, Y. X. Zeng, X. Tu, A. Bogaerts, *RSC Adv.* **2015**, *5*, 29799.
[38] Y. P. Zhang, Y. Li, Y. Wang, C. J. Liu, B. Eliasson, *Fuel Process. Technol.* **2003**, *83*, 101.
[39] A. J. Zhang, A. M. Zhu, J. Guo, Y. Xu, C. Shi, *Chem. Eng. J.* **2010**, *156*, 601.
[40] A. M. Huang, G. G. Xia, J. Y. Wang, S. L. Suib, Y. Hayashi, H. Matsumoto, *J. Catal.* **2000**, *189*, 349.
[41] Q. Chen, W. Dai, X. M. Tao, H. Yu, X. Y. Dai, Y. X. Yin, *Plasma Sci. Technol.* **2006**, *8*, 181.
[42] A. J. Wu, J. H. Yan, H. Zhang, M. Zhang, C. M. Du, X. D. Li, *International Journal of Hydrogen Energy* **2014**, *39*, 17656.
[43] M. W. Li, G. H. Xu, Y. L. Tian, L. Chen, H. F. Fu, *J. Phys. Chem. A* **2004**, *108*, 1687.
[44] V. Shapoval, E. Marotta, *Plasma Process. Polym.* **2015**, *12*, 808.
[45] P. Liu, X. S. Liu, J. Shen, Y. X. Yin, T. Yang, Q. Huang, D. Auerbach, A. W. Kleiyn, *Plasma Sci. Technol.* **2019**, *21*, 4.
[46] T. Yang, J. Shen, T. C. Ran, J. Li, P. Chen, Y. X. Yin, *Plasma Sci. Technol.* **2018**, *20*, 9.
[47] J. Li, X. Q. Zhang, J. Shen, T. C. Ran, P. Chen, Y. X. Yin, *J. CO2 Util.* **2017**, *21*, 72.
[48] J. A. Mucha, D. L. Flamm, D. E. Ibbotson, *J. Appl. Phys.* **1989**, *65*, 3448.
[49] Q. Huang, D. Y. Zhang, D. P. Wang, K. Z. Liu, A. W. Kleyn, *Journal of Physics D-Applied Physics* **2017**, *50*, 6.
[50] R. L. Yang, D. Y. Zhang, K. W. Zhu, H. L. Zhou, X. Q. Ye, A. W. Kleyn, Y. Hu, Q. Huang, *Acta Phys.-Chim. Sin.* **2019**, *35*, 292.
[51] S. V. T. Nguyen, J. E. Foster, A. D. Gallimore, *Rev. Sci. Instrum.* **2009**, *80*, 8.
[52] F. L. Tabares, D. Alegre, M. Mozetk, A. Vesel, *Nukleonika* **2012**, *57*, 287.
[53] X. Cao, Y. Xia, B. Chen, S. Tian, C. Wang, D. Yang, X. Xue, W. Zhang, J. Wang, F. Gou, Z. Zhu, W. Ou, S. Chen, *Plasma Sci. Technol.* **2015**, *17*, 20.